LIGHTCURVES AND SYNODIC ROTATION PERIODS FOR 23 ASTEROIDS FROM SOPOT ASTRONOMICAL OBSERVATORY: 2022 OCTOBER – 2023 JULY

Vladimir Benishek
Belgrade Astronomical Observatory
Volgina 7, 11060 Belgrade 38, SERBIA
vlaben@yahoo.com

(Received: 2023 July 15)

Lightcurve and synodic rotation period results were derived using photometric data for 23 asteroids obtained at the Sopot Astronomical Observatory in the time span 2022 October – 2023 July.

Photometric observations of 23 asteroids were conducted at Sopot Astronomical Observatory (SAO) from 2022 October through 2023 July in order to determine the asteroids' synodic rotation periods. For this purpose, two 0.35-m *f*/6.3 Meade LX200GPS Schmidt-Cassegrain telescopes were employed. The telescopes are equipped with a SBIG ST-8 XME and a SBIG ST-10 XME CCD cameras. The exposures were unfiltered and unguided for all targets. Both cameras were operated in 2×2 binning mode, which produces image scales of 1.66 arcsec/pixel and 1.25 arcsec/pixel for ST-8 XME and ST-10 XME cameras, respectively. Prior to measurements, all images were corrected using dark and flat field frames.

Photometric reduction was conducted using *MPO Canopus* (Warner, 2018). Differential photometry with up to five comparison stars of near solar color ($0.5 \leq$ B-V ≤ 0.9) was performed using the Comparison Star Selector (CSS) utility. This helped ensure a satisfactory quality level of night-to-night zero-point calibrations and correlation of the measurements within the standard magnitude framework. Field comparison stars were calibrated using standard Cousins R magnitudes derived from the Carlsberg Meridian Catalog 15 (VizieR, 2023) Sloan r' magnitudes using the formula: R = r' - 0.22 in all cases presented in this paper. In some instances, small zero-point adjustments were necessary in order to achieve the best match between individual data sets in terms of achieving the most favorable statistical indicators of Fourier fit goodness.

Lightcurve construction and period analysis was performed using *Perfindia* custom-made software developed in the R statistical programming language (R Core Team, 2020) by the author of this paper. The essence of its algorithm is reflected in finding the most favorable solution for rotational period by minimizing the *residual standard error* of the lightcurve Fourier fit.

The lightcurve plots presented in this paper show so-called 2% error for rotational periods, i.e., an error that would cause the last data point in a combined data set by date order to be shifted by 2% (Warner, 2012) and represented by the following formula:

$$\Delta P = (0.02 \cdot P^2) / T$$

where P and T are the rotational period and the total time span of observations, respectively. Both of these quantities must be expressed in the same units.

Table I gives the observing circumstances and results.

615 Roswitha. A low-amplitude (0.09 mag) rotational lightcurve obtained over three nights spanning nearly a month from early 2023 February to early 2023 March shows no substantial change in shape during that time. The SAO observations indicate a fairly unambiguous solution for a synodic rotation period of $P = 4.3902 \pm 0.0006$ h, which is quite close to the two previously known period determinations found in the Asteroid Lightcurve Database (LCDB; Warner et al., 2009): 4.422 h by Shevchenko et al. (2008) and 4.42 h by Behrend (2021web).

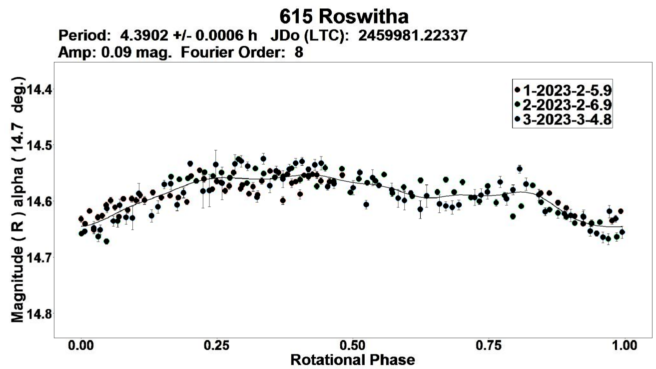

1346 Gotha. A large number of previous rotation period determination results from the LCDB, such as the following: 2.64067 h by Behrend (2011web), Waszczak et al. (2015, 2.640 h), Aznar Macias (2017, 2.642 h), Benishek (2022a, 2.640 h) match well with the bimodal period of $P = 2.639 \pm 0.002$ h, found from the 2023 May SAO observations obtained over two nights.

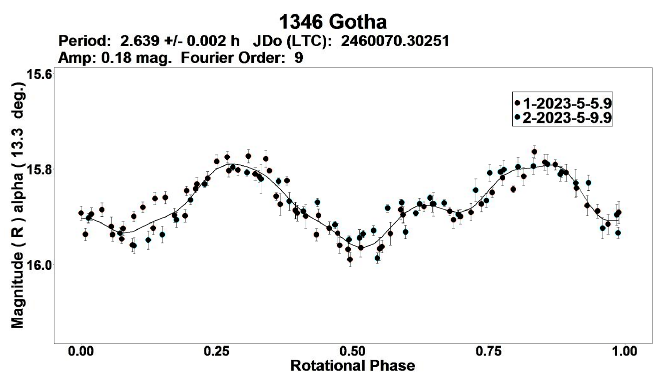

1394 Algoa. Observations conducted over two consecutive nights in 2023 July show an unequivocal bimodal period of $P = 2.769 \pm 0.006$ h, statistically equal to virtually all previous results listed in the LCDB, some of which are as follows: Hills (2012, 2.768 h), Klinglesmith et al. (2013, 2.768 h), Behrend (2020web, 2.76829 h).

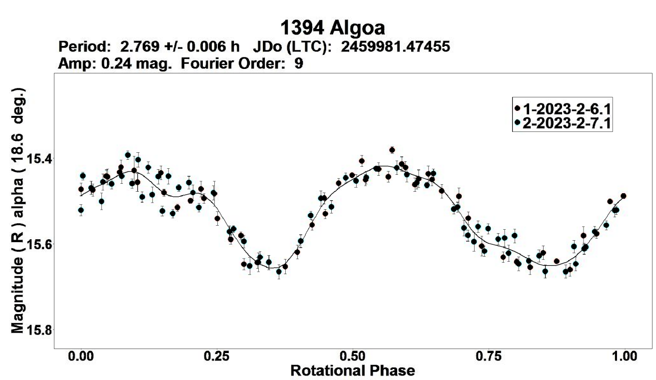

1627 Ivar. A dense photometric dataset obtained over two consecutive nights in 2023 May shows an unambiguous large-amplitude (0.68 mag.) bimodal rotation period solution of $P = 4.79 \pm 0.02$ h, a value in excellent agreement with 20 synodic and 3 sidereal previous rotation period values for this NEA ranging between 4.7947 an 4.801 hours and determined in the time span from 1985 to 2020 (LCDB; Warner et al., 2009).

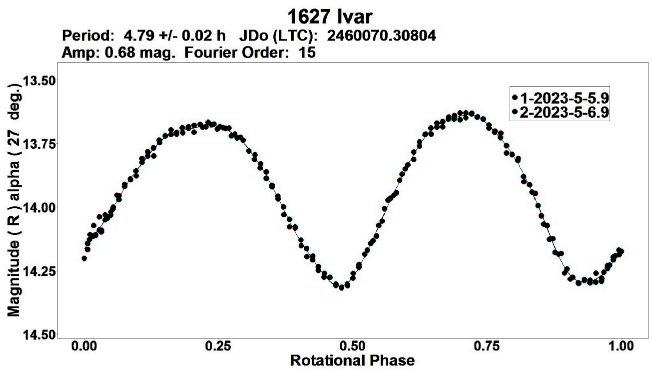

1925 Franklin-Adams. A bimodal solution for period of $P = 2.9783 \pm 0.0002$ h was found from a dense combined dataset acquired at SAO over 10 nights from late 2023 May through early July. The obtained result is well consistent with the prior period determinations by Warner (2013a, 2.978 h), Waszczak et al. (2015, 2.979 h) and a sidereal period result by Hanuš et al. (2016, 2.978301 h).

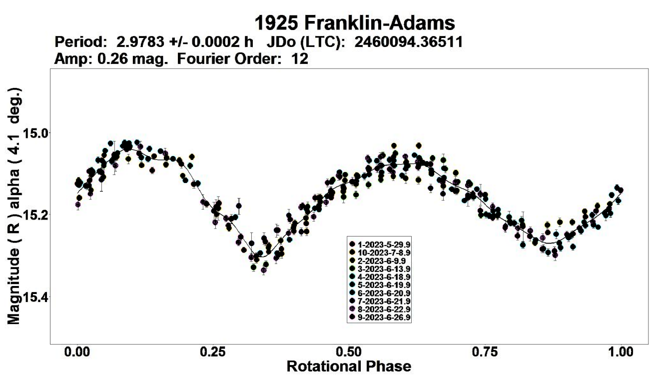

1929 Kollaa. Observations of this V-type asteroid from late 2023 March carried out at SAO over three nights yielded a bimodal period result of $P = 2.989 \pm 0.002$ h, which is well consistent with previous findings listed in the LCDB: 2.9887 h (Behrend, 2008web), 2.982 h (Benishek, 2022b).

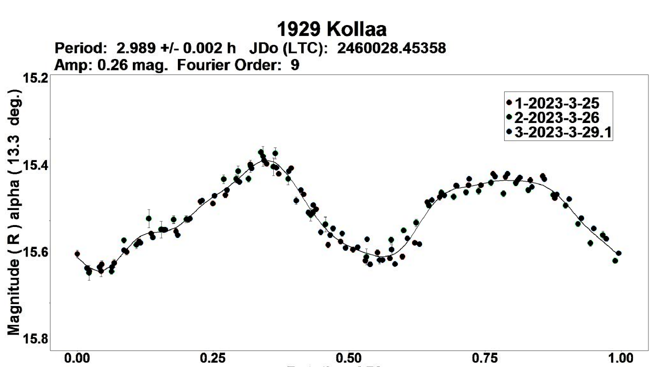

2034 Bernoulli. Data collected on three nights in early 2023 February yielded a bimodal solution for a period of $P = 6.252 \pm 0.005$ h. This value does not differ much from the previously determined fairly uniform results by Alkema (2013, 6.248 h), McNeill et al. (2019, 6.245 h), Pal et al. (2020, 6.24919 h), and Benishek (2021, 6.249 h).

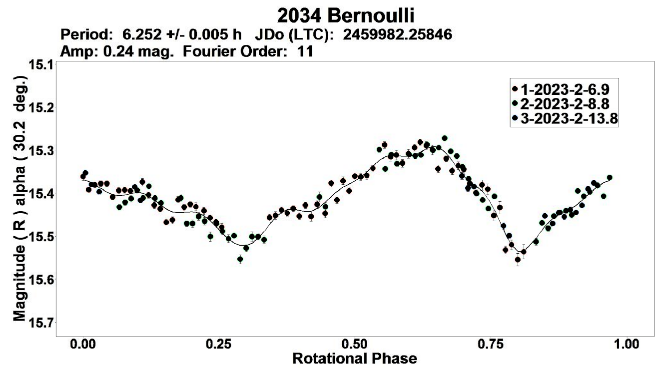

3628 Boznemcova. The only prior rotation period determination from Warner (2008, 3.335410 h) matches well the bimodal result ($P = 3.3352 \pm 0.0008$ h) found from the 2023 June SAO data collected on five nights.

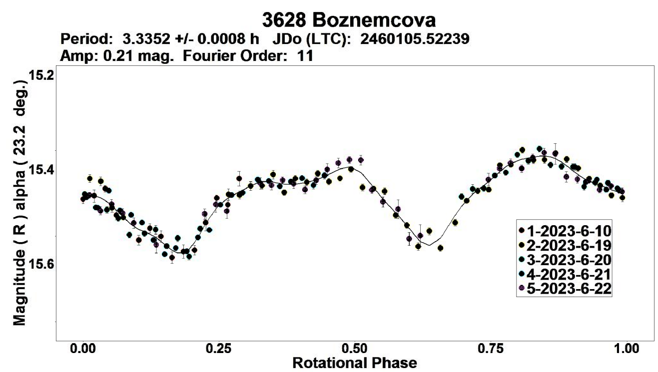

4353 Onizaki. An unambiguous bimodal period ($P = 4.43 \pm 0.02$ h) was derived from the data obtained on two consecutive nights in 2023 February. Several previously determined periods listed in the LCDB are also in the range of 4.429 h to 4.49 h.

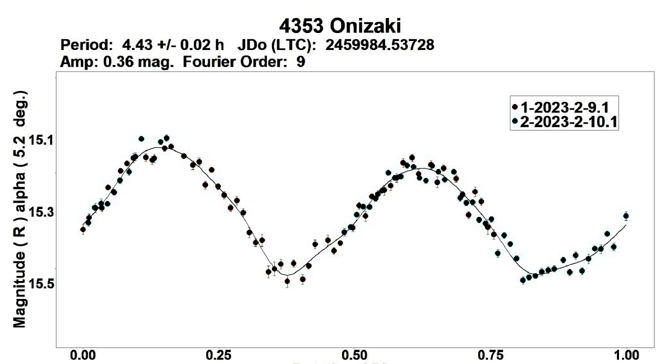

4497 Taguchi. Period result ($P = 3.5635 \pm 0.0009$ h) established from the 2023 January data obtained over three nights is consistent with the vast majority of previous period determinations, some of which are as follows: 3.563 h (Almeida et al., 2004), 3.567 h (Behrend, 2012web), 3.563 h (Warner, 2013b), 3.5639 h (Pal et al., 2020).

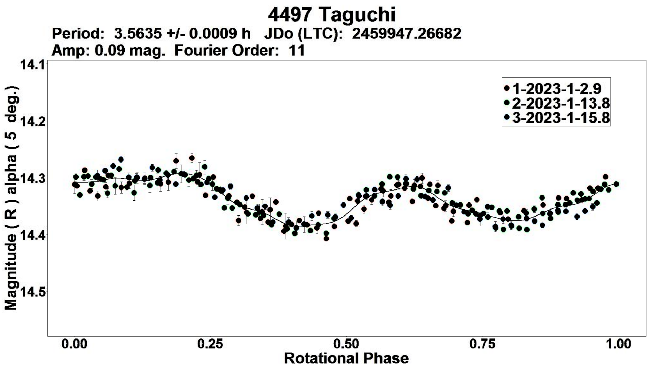

4572 Brage. The only prior rotation period result from Behrend (2015, 2.99105 h) is virtually identical to the bimodal period solution derived from the 2023 April-May SAO data (P = 2.9910 ± 0.0004 h).

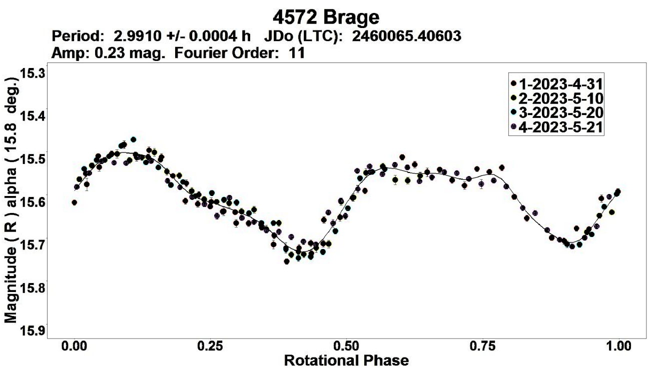

5962 Shikokutenkyo. There is no information on previous rotation period determinations for this asteroid in the LCDB. Period analysis performed on the dense combined dataset from four nights in 2023 April - May indicates an unequivocal period solution of P = 3.8959 ± 0.0005 h, associated with a rather large amplitude (0.38 mag.) bimodal lightcurve at relatively low solar phase angles.

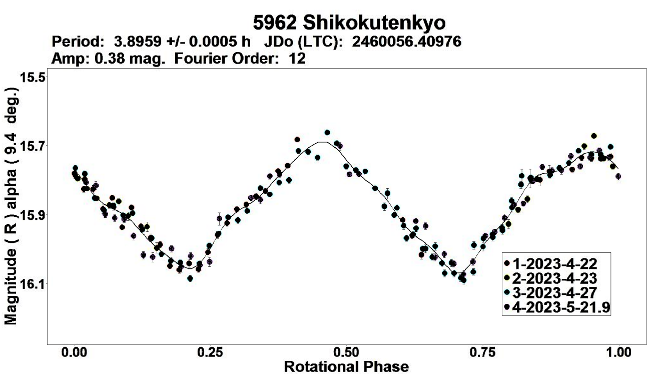

6667 Sannaimura. The only prior rotation period result by Pal et al. (2020, 2.89282 h) is almost identical to the statistically most favorable period of P = 2.8922 ± 0.0004 h, obtained from the analysis conducted on the SAO photometric data obtained on five nights in 2023 March.

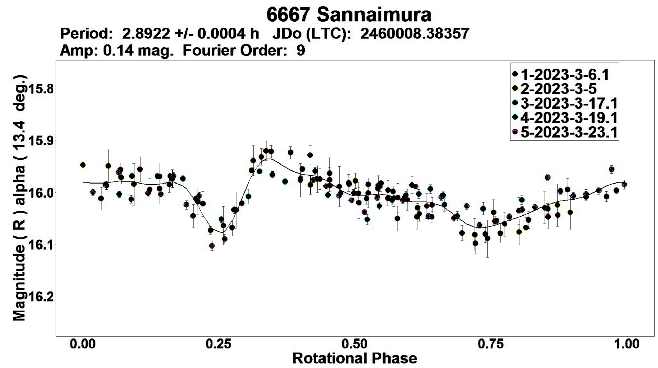

(6896) 1987 RE1. There are no previous rotation period results present in the LCDB. Data collected in 2022 October-November over five nights indicate a period of P = 3.4414 ± 0.0004 h as the most favorable solution.

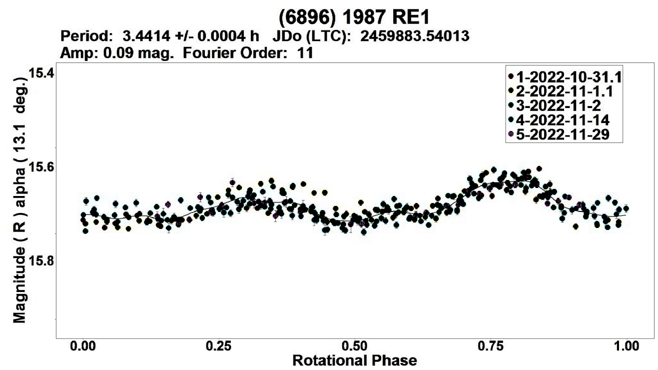

8548 Sumizihara. Observations of this asteroid carried out in early 2023 January (Benishek, 2023) were continued during 2023 February and led to a bimodal solution for a rotation period of P = 3.1906 ± 0.0007 h, close to the one obtained from the 2023 January data (3.187 h). The new result is also in line with all previous period determinations cited in the LCDB, which are in the range between 3.187 and 3.195 hours.

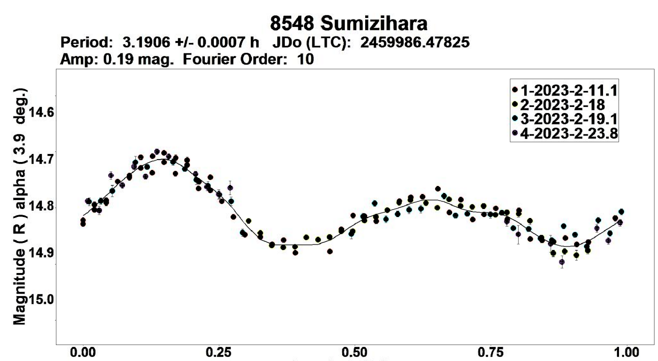

10646 Machielalberts. Waszczak et al. (2015) found a value of 3.058 h for a rotation period. A bimodal solution of P = 2.969 ± 0.004 h was determined from the SAO data taken over two nights in 2023 March.

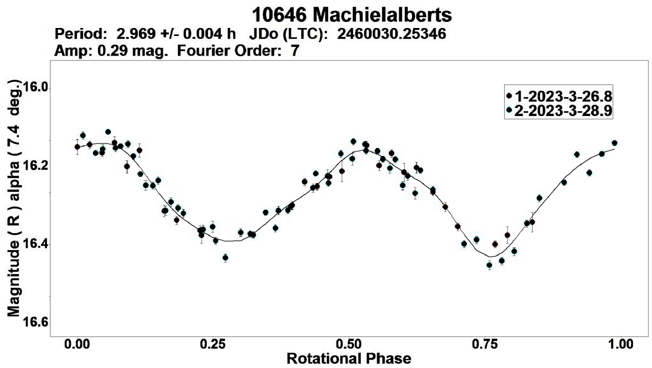

(13166) 1995 WU1. Data obtained in 2023 February led to a bimodal period solution of $P = 3.82 \pm 0.02$ h. The previously found values are in good accordance with the newly established result: 3.8123 h (Pravec, 2008web), 3.8101 h (Pravec, 2010web), 3.810 h (Waszczak et al., 2015), 3.8104 h (Pravec, 2019web).

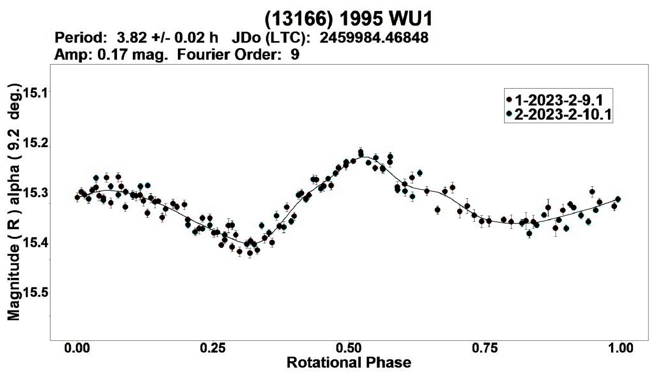

(15473) 1999 BL9. A high concordance is apparent between the only previously rotation period determination by Pal et al. (2020, 4.46844 h) and the bimodal result found from the 2023 February SAO data ($P = 4.467 \pm 0.002$ h).

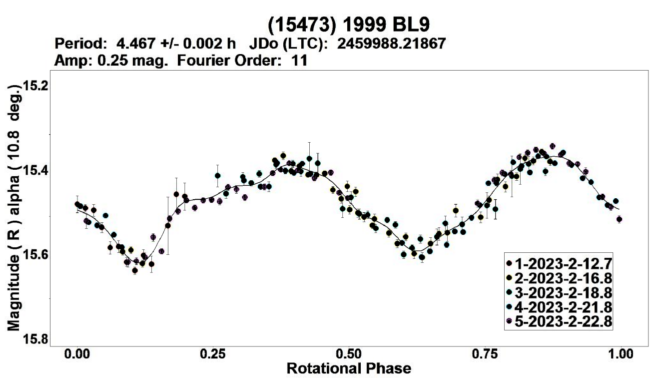

(23080) 1999 XH100. Similar to the previous case, the bimodal period solution of $P = 3.0627 \pm 0.0003$ h derived from SAO data collected over 10 nights in 2023 April-May shows an exact match (within the period error bounds) with the only previous result by Pal et al. (2020, 3.06273 h).

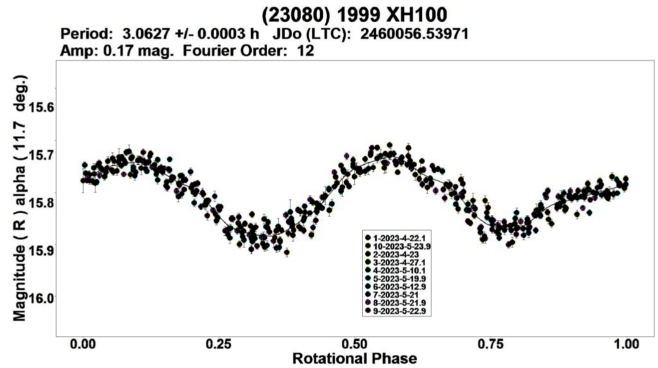

26355 Grueber. Data from two nights in 2023 January at low solar phase angles show a fairly high-amplitude (0.63 mag.) bimodal lightcurve phased to a period of $P = 4.540 \pm 0.009$ h as a unique solution. This result is in very good agreement with the previous results by Fauerbach and Fauerbach (2019, 4.539 h), Behrend (2020, 4.541 h), as well as a sidereal value determined by Ďurech et al. (2019, 4.540231 h).

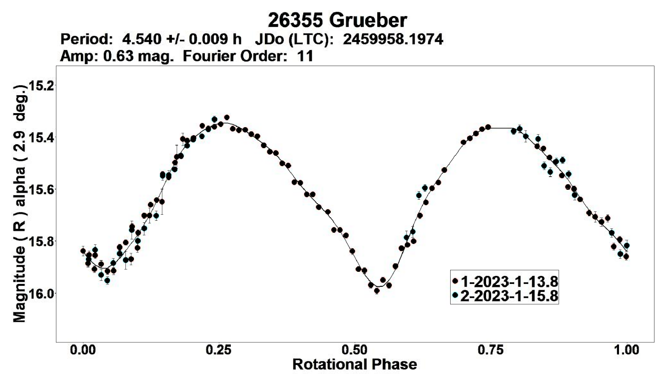

(27290) 2000 AM127. No rotation period determination results were previously known. An equivocal bimodal period solution of $P = 3.5719 \pm 0.0004$ h was found from the dense combined dataset acquired over four nights in 2023 March - April.

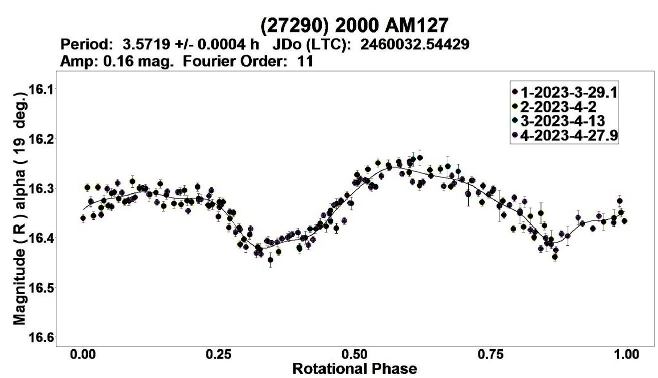

(66469) 1999 RL18. Pal et al. (2020) found a period of 2.86509 h. A very close value to this previous one ($P = 2.864 \pm 0.006$ h) was found from the 2023 March SAO data obtained on two consecutive nights.

Number	Name	20yy/mm/dd	Phase	L_{PAB}	B_{PAB}	Period (h)	P.E.	Amp	A.E.	Grp
615	Roswitha	23/02/05-23/03/04	14.7,19.4	97	3	4.3902	0.0006	0.09	0.03	MB-M
1346	Gotha	23/05/05-23/05/09	13.3,14.4	190	9	2.639	0.002	0.18	0.03	EUN
1394	Algoa	23/02/05-23/02/07	18.6,18.3	182	0	2.769	0.006	0.24	0.02	MB-I
1627	Ivar	23/05/05-23/05/07	27.0,27.4	194	13	4.79	0.02	0.68	0.01	NEA
1925	Franklin-Adams	23/05/29-23/07/08	*4.1,15.2	253	6	2.9783	0.0002	0.26	0.02	MB-I
1929	Kollaa	23/03/24-23/03/29	13.3,11.5	208	7	2.989	0.002	0.26	0.02	V
2034	Bernoulli	23/02/06-23/02/13	30.2,31.0	84	11	6.252	0.005	0.24	0.02	MB-I
3628	Boznemcova	23/06/10-23/06/22	23.2,19.6	299	7	3.3352	0.0008	0.21	0.02	MB-I
4353	Onizaki	23/02/09-23/02/10	5.2, 5.2	142	11	4.43	0.02	0.36	0.03	MB-I
4497	Taguchi	23/01/02-23/01/15	*5.0, 4.3	109	4	3.5635	0.0009	0.09	0.02	MB-I
4572	Brage	23/04/30-23/05/21	15.8, 9.5	248	13	2.9910	0.0004	0.23	0.02	MB-I
5962	Shikokutenkyo	23/04/21-23/05/22	*9.4, 7.8	228	9	3.8959	0.0005	0.38	0.03	EUN
6667	Sannaimura	23/03/04-23/03/23	14.0, 4.9	189	2	2.8922	0.0004	0.14	0.04	MB-I
6896	1987 RE1	22/10/31-22/11/29	*13.1,8.4	56	7	3.4414	0.0004	0.09	0.02	MB-I
8548	Sumizihara	23/02/10-23/02/23	*3.9, 4.5	148	1	3.1906	0.0007	0.19	0.02	MB-I
10646	Machielalberts	23/03/26-23/03/29	7.4, 8.6	173	-1	2.969	0.004	0.29	0.03	MB-I
13166	1995 WU1	23/02/08-23/02/10	9.2, 9.0	147	16	3.82	0.02	0.17	0.02	MB-I
15473	1999 BL9	23/02/12-23/02/22	10.8,13.7	131	-16	4.467	0.002	0.25	0.02	MB-I
23080	1999 XH100	23/04/22-23/05/24	-11.7, 7.9	231	10	3.0627	0.0003	0.17	0.02	MB-M
26355	Grueber	23/01/13-23/01/15	2.9, 3.7	109	5	4.540	0.009	0.63	0.03	MB-I
27290	2000 AM127	23/03/29-23/04/28	19.0,11.1	219	16	3.5719	0.0004	0.16	0.02	MB-I
66469	1999 RL18	23/03/16-23/03/18	5.5, 6.1	165	-4	2.864	0.006	0.24	0.05	MAR
67934	2000 WY133	23/02/13-23/02/16	12.6,14.0	119	-6	9.12	0.03	1.07	0.06	EUN

Table I. Observing circumstances and results. Phase is the solar phase angle given at the start and end of the date range. If preceded by an asterisk, the phase angle reached an extrema during the period. L_{PAB} and B_{PAB} are the average phase angle bisector longitude and latitude. Grp is the asteroid family/group (Warner et al., 2009): EUN = Eunomia, MB-I/M = main-belt inner /middle, NEA = near-Earth asteroid, MAR = Maria, V = Vestoid.

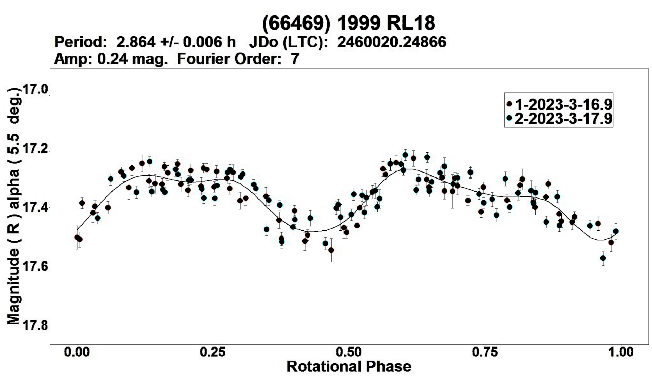

(67934) 2000 WY133. A Eunomia family member with no previously determined rotation period. A bimodal lightcurve with an extremely high amplitude of over one magnitude indicating an elongated shape and a rotation period of $P = 9.12 \pm 0.03$ h results from the 2023 February data gathered on three nights.

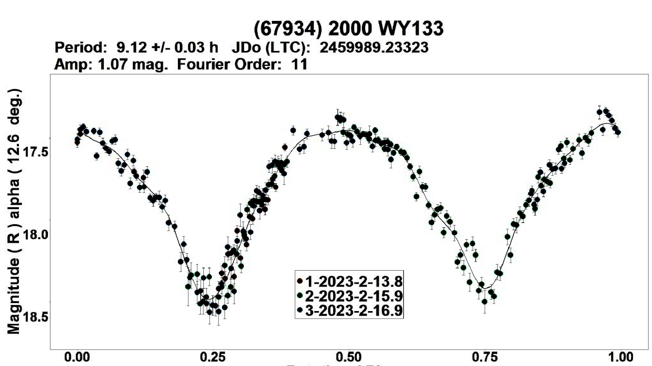

Acknowledgements

Observational work at Sopot Astronomical Observatory is generously supported by Gene Shoemaker NEO Grants awarded by the Planetary Society in 2018 and 2022.

References

Alkema, M.S. (2013). "Asteroid Lightcurve Analysis at Elephant Head Observatory: 2012 November - 2013 April." *Minor Planet Bull.* **40**, 133 - 137.

Almeida, R.; Angeli, C.A.; Duffard, R.; Lazzaro, D. (2004). "Rotation periods for small main-belt asteroids." *A&A* **415**, 403 - 406.

Aznar Macias, A. (2017). "Lightcurve Analysis from APT Observatory Group for Nine Mainbelt Asteroids: 2016 July - September. Rotation Period and Physical Parameters." *Minor Planet Bull.* **44**, 60 - 63.

Behrend, R. (2008web, 2011web, 2012web, 2015web, 2020web, 2021web). Observatoire de Geneve web site. *http://obswww.unige.ch/~behrend/page_cou.html*

Benishek, V. (2021). "Photometry of 30 Asteroids at Sopot Astronomical Observatory: 2020 February - October." *Minor Planet Bull.* **48**, 77 - 83.

Benishek, V. (2022a). "CCD Photometry of 35 Asteroids at Sopot Astronomical Observatory: 2021 November - 2022 July." *Minor Planet Bull.* **49**, 333 - 341.

Benishek, V. (2022b). "CCD Photometry of 11 Asteroids at Sopot Astronomical Observatory: 2021 July - 2022 January." *Minor Planet Bull.* **49**, 149 - 152.

Benishek, V. (2023). "Lightcurves and Synodic Rotation Periods for 17 Asteroids from Sopot Astronomical Observatory: 2022 June - 2023 January." *Minor Planet Bull.* **50**, 142 - 147.

Ďurech, J.; Hanuš, J.; Vančo, R. (2019). "Inversion of Asteroid Photometry from Gaia DR2 and the Lowell Observatory Photometric Database." *A&A* **631**, id. A2, 4 pp.

Fauerbach, M.; Fauerbach, M. (2019). "Lightcurve Analysis of Asteroids 131 Vala, 1184 Gaea, 7145 Linzexu, and 26355 Grueber." *Minor Planet Bull.* **46**, 236 - 237.

Hanuš, J.; Ďurech, J.; Oszkiewicz, D.A.; Behrend, R.; Carry, B.; and 1643 colleagues (2016). "New and updated convex shape models of asteroids based on optical data from a large collaboration network." *Astronomy & Astrophysics* **586**, A108.

Hills, K. (2012). "Asteroid Lightcurve Analysis at Riverland Dingo Observatory: 1394 Algoa, 1660 Wood, 8882 Sakaetamura, and (15269) 1990 XF." *Minor Planet Bull.* **39**, 239 - 240.

Klinglesmith, D.A., III.; Risley, E.; Turk, J.; Vargas, A.; Warren, C. (2013). "Lightcurves for 1394 Algoa, 3078 Horrocks, 4724 Brocken, 6329 Hikonejyo from Etscorn Campus Observatory." *Minor Planet Bull.* **40**, 16 - 17.

McNeill, A.; Mommert, M.; Trilling, D.E.; Llama, J.; Skiff, B. (2019). "Asteroid Photometry from the Transiting Exoplanet Survey Satellite: A Pilot Study." *Astron. J. Suppl. Series* **245**, article id. 29.

Pal, A.; Szakáts, R.; Kiss, C.; Bódi, A.; Bognár, Z.; Kalup, C.; Kiss, L.L.; Marton, G.; Molnár, L.; Plachy, E.; Sárneczky, K.; Szabó, G.M.; Szabó, R. (2020). "Solar System Objects Observed with TESS - First Data Release: Bright Main-belt and Trojan Asteroids from the Southern Survey." *Ap. J. Supl. Ser.* **247**, 26 - 34.

Pravec, P. (2008web, 2010web, 2019web). Photometric Survey for Asynchronous Binary Asteroids web site. *http://www.asu.cas.cz/~ppravec/newres.txt*

R Core Team (2020). R: A language and environment for statistical computing. R Foundation for Statistical Computing. Vienna, Austria. *https://www.R-project.org/*

Shevchenko, V.G.; Chiorny, V.G.; Gaftonyuk, N.M.; Krugly, Y.N.; Belskaya, I.N.; Tereschenko, I.A.; Velichko, F.P. (2008). "Asteroid observations at low phase angles. III. Brightness behavior of dark asteroids." *Icarus* **196**, 601 - 611.

VizieR (2023). *http://vizier.u-strasbg.fr/viz-bin/VizieR*

Warner, B.D. (2008). "Asteroid Lightcurve Analysis at the Palmer Divide Observatory: June - October 2007." *Minor Planet Bull.* **35**, 56 - 60.

Warner, B.D.; Harris, A.W.; Pravec, P. (2009). "The Asteroid Lightcurve Database." *Icarus* **202**, 134-146. Updated 2021 Dec 14. *http://www.minorplanet.info/lightcurvedatabase.html*

Warner, B.D. (2012). *The MPO Users Guide: A Companion Guide to the MPO Canopus / PhotoRed Reference Manuals*. BDWPublishing, Eaton, CO.

Warner, B.D. (2013a). "Asteroid Lightcurve Analysis at the Palmer Divide Observatory: 2013 January - March." *Minor Planet Bull.* **40**, 137 - 145.

Warner, B.D. (2013b). "Asteroid Lightcurve Analysis at CS3-Palmer Divide Station: 2013 May - June." *Minor Planet Bull.* **40**, 208 - 212.

Warner, B.D. (2018). MPO Canopus software, version 10.7.11.3. *http://www.bdwpublishing.com*

Waszczak, A.; Chang, C.-K.; Ofek, E.O.; Laher, R.; Masci, F.; Levitan, D.; Surace, J.; Cheng, Y.-C.; Ip, W.-H.; Kinoshita, D.; Helou, G.; Prince, T.A.; Kulkarni, S. (2015). "Asteroid Light Curves from the Palomar Transient Factory Survey: Rotation Periods and Phase Functions from Sparse Photometry." *Astron. J.* **150**, A75.